Archimedes screw generator powerplant assessment and field measurement campaign

Scott Simmons, Chris Elliott, Mike Ford, Adrian Clayton, and William David Lubitz

Published as:

Simmons SC, Elliott C, Ford M, Clayton A, Lubitz WD. Archimedes screw generator powerplant assessment and field measurement campaign. Energy for Sustainable Development. 2021 Dec 1;65:144-61.

Abstract

The Archimedes screw generator (ASG) is a cost-effective, eco-friendly micro-hydropower technology that can operate effectively in low head and moderate flow rate environments. The technology is well suited for distributed micro-hydropower and off-grid energy schemes, and its simple, robust design allows for local manufacturing and installation in developing regions. There are many successful ASG powerplants installed on- and off-grid, particularly in Europe. Archimedes screw generators are largely designed by experience. As such, there is a need for an accurate performance model in the literature to optimize plant design. There is a lack of experimental data in the literature, particularly for large-scale, real-world screw plants. This study sought to gather both qualitative and quantitative data and introduce it to the literature. The authors surveyed and measured various Archimedes screw powerplants in the United Kingdom. The measurements were then added to a larger dataset to validate a CFD simulation across a range of screw sizes: from a small 15 cm diameter laboratory screw to a large 3.5 m diameter powerplant. The authors plan to use the CFD simulation's accurate approximations to further the literature's ASG performance data for a wide range of screw sizes, shapes, and operational parameter.

19 ## Keywords

20 Archimedes screw generator, Reverse Archimedes screw, hydrodynamic screw, micro-hydropower, off-

21 grid electrification, run-of-river, diversion hydropower

22 ## Notation

23 *The following symbols are used in this paper:*

D_i = inner diameter of screw (m);
D_o = outer diameter of screw (m);
g = gravitational constant (m/s^2)
G_w = blade-trough gap width (m)
H = head (m);
h_L = lower water level (m);
h_U = upper water level (m);
L = flighted length of screw (m);
N = number of blades of screw (-);
P = rated power (W);
P_e = electrical power produced (W);
P_s = mechanical power converted by the screw (W);
Q = flow rate (m^3/s);
S = screw pitch (m);
T = mechanical torque at the screw shaft (W);
z_{wl} = bucket water level (m);
β = inclination angle of screw (°);
η = mechanical efficiency of screw (-)
ρ = density of working fluid (i.e. water) (kg/m^3)
ψ_L = lower submergence level (-)
Ω = rotation speed (rev/min);

24 ## 1. Introduction

25 Archimedes screws are an ancient pumping technology that have also been used to generate

26 hydropower since the 1990s [1]. An Archimedes screw is made up of a helical array of simple blades

27 wrapped around a central, cylindrical tube – like a wood screw. In a power generating mode, the screw

rotates in the reverse direction that would be used for pumping, and hydro-electric energy is generated mostly due to the static pressure differences on the screw blades (or "flights") (Fig. 1); it is common to refer to the technology as an Archimedes screw generator (ASG), or less commonly as a reverse Archimedes screw (RAS) during this type of operation. Due to their simple, robust design ASGs are an eco-friendly, low cost hydropower technology [2–4], well suited for installation in developing regions.

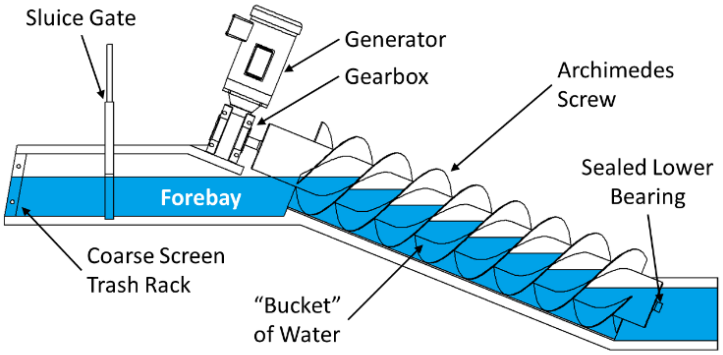

Figure 1: Diagram of typical Archimedes screw generator installation.

Rural, developing regions have little access to electricity. For example, only about 45% of the rural population of Sub-Saharan Africa had access to electricity in 2018 [5]; an increase from 29% in 2009, but still low [6]. Access to electricity is a priority for rural Cameroonians [7] as it provides increased health, security, and productivity. It also gives better access to information, education, and entertainment [8]. Electricity reduces reliance on fossil fuels like diesel and kerosene by eliminating the need for kerosene-based lanterns and wood-fueled cookstoves. An estimated 3 billion people worldwide cook using wood biomass cookstoves or open fires; close to 4 million people die per year due to illness attributable to indoor air pollution from these methods [9].

There was an estimated 30.4 GW of installed hydropower capacity in Sub-Saharan Africa in 2017 [10], however, 92% of an estimated 300 GW of potential is untapped [11]. Local availability and capital expenses tend to be major hurdles in developing hydropower installations in rural developing regions [7]. Equipment must either imported or manufactured locally. Imported systems tend to be more

47 sophisticated (by way of experience), but very costly to import and install. It can be very difficult for
48 local technicians to maintain complex imported systems, with access to parts being a particular issue.
49 Ho-yan et al. (2014) noted non-operational hydropower systems in Cameroon that could not be repaired
50 locally due to lack of experience or inability to access replacement parts [7]. The local manufacturing of
51 equipment and implementation of less complex technologies, such as Archimedes screw generator
52 which do not require precision machining, would mitigate many of these issues. Further, many ASGs
53 have been successfully retrofit to existing mill sites or flood control structures to reduce cost of civil
54 works [12].

55 The majority of active ASG powerplants are in the developed world, predominantly in Europe [13].
56 However, some ASGs have been successfully implemented for rural electrification in the developing
57 world. The town of Erijiyan, Nigeria is supplied with an average of 83 kW from a 3-bladed screw at the
58 nearby Arinta waterfall [14]. Okamura et al. (2015) proposed a pico-scale, off-grid ASG system to power
59 48 homes of a village in southern Tanzania. They proposed that the system be designed, manufactured,
60 and installed by locally-based companies to reduce costs and improve familiarity with the technology
61 [15]. The literature contains a French-language publication discussing modelling, development, and
62 testing of ASGs for use in typical waterfalls in the Democratic Republic of Congo [16].

63 It was suggested that ASGs are good candidates for distributed microhydro scenarios. In some
64 developing countries there is a recognition of the need for more decentralized power generation [17].
65 There are also successful examples of hydropower community groups that may serve as a model for
66 future developments; the hydropower scheme at Ruswarp (UK) is successfully operated by the local
67 Whitby Esk Energy community group.

68 The precedents set by existing installations in the developed and developing world can help to
69 optimize the performance of Archimedes screw generator powerplants – improving efficiency and

reducing cost by experience. This article explores three successful ASG hydropower schemes to evaluate their performance, documenting data that is crucial for future model developments.

1.1. Archimedes screw generators

Archimedes screw plants are small-scale hydropower plants that usually operate as diversion (or "run-of-river") schemes. Traditionally, ASGs operate at sites with low head ($H < 3.5\ m$) and moderate flow rates ($Q = 0.25\ to\ 5\ m^3/s$) [3][18] (Fig. 2). However, more recent plants have installed and operated much larger screws successfully, suggesting that this operating envelope could be extended to include heads of about $H = 5\ m$, and flow rates up to about $Q = 15\ m^3/s$ [19]. For comparison, the operating envelope of ASGs is plotted with other common hydro-electric technologies in Fig. 2, including: Cross-flow, Kaplan, Francis, Pelton, Turgo, and Very Low Head (VLH) turbines, as well as undershot, overshot, and breast-shot waterwheels. Some real-world example powerplants are highlighted on the plot for reference, with details provided in Table 1.

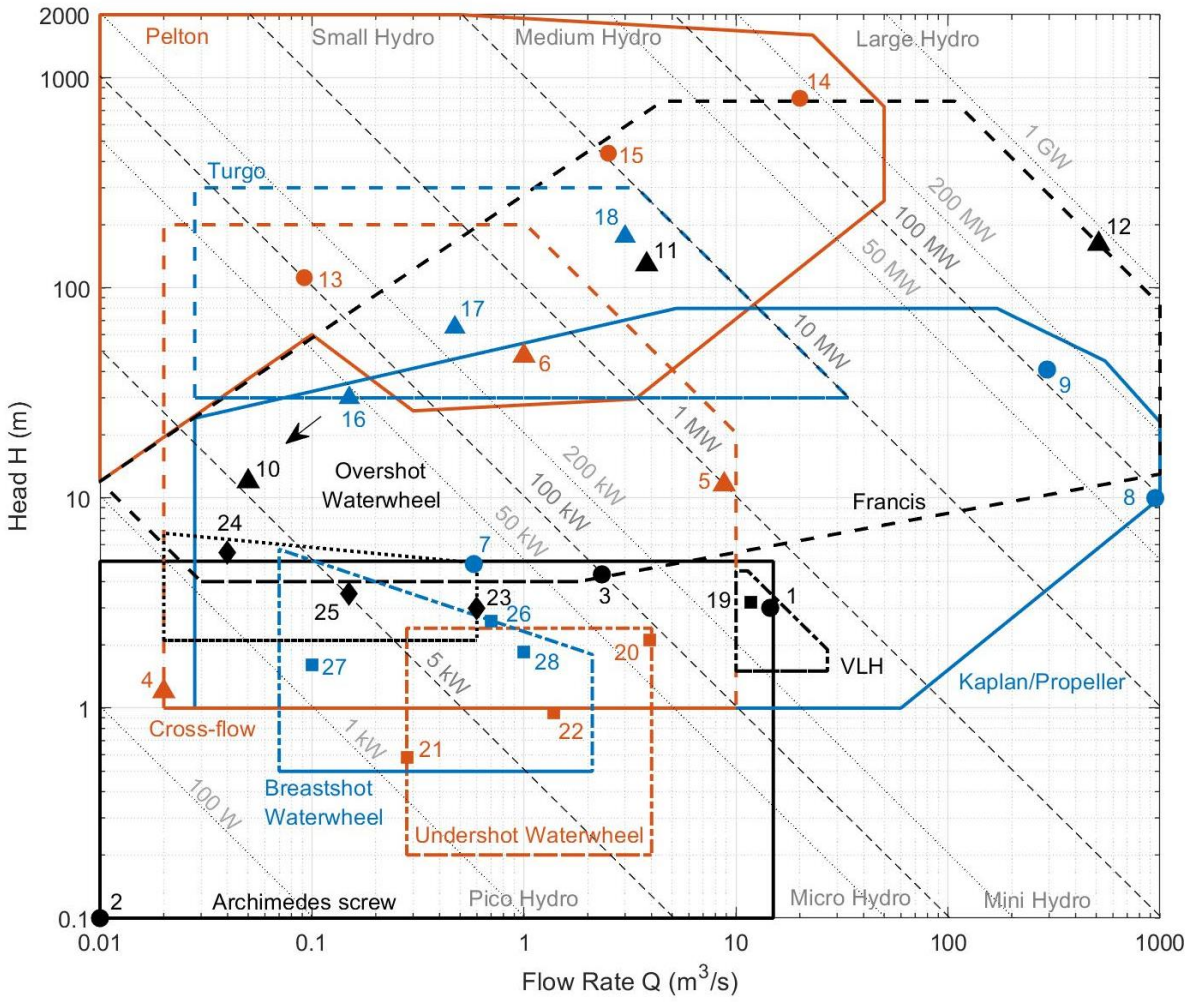

Figure 2: Operational ranges of various hydro-generating technologies [18]. Solid lines indicate the operating envelope, the coloured dots are examples of the operating points of example hydropower plants. Data from various sources [20,21,30–39,22,40–44,23–29].

Hydro turbines are often distinguished as either reaction or impulse turbines. Reaction turbines produce torque due to the pressure variations in a moving fluid, as such they tend to be used for larger-scale systems with higher flow rates and comparatively lower head. Francis turbines and propeller-type turbines are examples of reaction turbines. The Kaplan turbine is the most common variant of propeller-type turbines, and the very low head (VLH) turbine is a variant of the Kaplan turbine that is used for low head hydro sites. Impulse turbines generate torque by converting the impulse of a moving fluid into mechanical motion. They utilize comparatively high heads and correspondingly high static pressure differences to produce a high velocity fluid jet in the turbine; the high velocity fluid imparts its

momentum on the turbine rotor. Examples of common impulse turbines include Pelton, Turgo, and Cross-flow turbines.

Neither waterwheels nor ASGs are hydro turbines since they are not enclosed in pressure casings and do not use the same momentum mechanisms to convert fluid pressure into mechanical energy. Rather, both the screws and waterwheels compartmentalize water into discrete volume ("buckets") and convert the static pressure of the bulk volume into mechanical power.

Table 1 provides more details of the example power plants defined in Fig. 2. Generally, three sites were shown for each device on the figure to provide the context of a comparatively large, moderate, and small instance of each device.

Table 1: Index of example hydropower plants from Fig. 2. Turbine types are identified as follows: Archimedes screw generators (A), Crossflow turbines (C), Kaplan/Propeller type turbines (K), Francis turbines (F), Pelton turbines (P), Turgo turbines (T), VLH turbines (V), Undershot waterwheels (U), Overshot waterwheels (O), and Breast-shot waterwheels (B). Data from various sources [20,21,30–39,22,40–44,23–29].

Site Number	Turbine Type	Site Identification	City	Country	Q (m^3/s)	H (m)	Reference
1	A	Widdington	Linton-on-Ouse	UK	14.5	3	https://www.landustrie.nl/
2	A	PicoPica	Ena	Japan	0.01	0.1	http://www.unido.or.jp/en/technology_db/5276/
3	A	Buckfast Abbey	Buckfastleigh	UK	2.33	4.33	https://www.renewablesfirst.co.uk/
4	C	Universiti Kebangsaan Malaysia	Bangi	Malaysia	0.02	1.2	Razak et al. (2010)
5	C	Elora	Elora	Canada	8.8	11.6	http://www.ossbergerhydro.com/projects.html
6	C	Aspen	Aspen	Colorado	1	47.5	http://www.ossbergerhydro.com/projects.html
7	K	Novarina	-	-	0.58	4.85	Quaranta (2020)
8	K	Engineer Sérgio Motta Dam	São Paulo	Brazil	950	10	https://www.ge.com/renewableenergy/
9	K	Peixe Angical	Peixe	Brazil	293.3	40.9	http://voith.com/
10	F	HS Dynamic	Hong Kong	China	0.05	12	https://www.hs-dynamics.com/
11	F	Candelaria	Chisec	Guatemala	3.79	129.45	https://www.gilkes.com/
12	F	Jhimuk Hydropower Plant	Khaira	Nepal	513.9	162	https://nwrmap.info/hydropower/
13	P	Blair Castle	Blair Atholl	UK	0.092	112	https://www.gilkes.com/
14	P	La Esmeralda Dam	Chivor	Columbia	20	800	https://www.hydropower.org/case-studies/
15	P	Hidroelectrica Choloma S.A	Guatemala City	Guatemala	2.5	438	https://www.gilkes.com/
16	T	Balbeg	Inverness	UK	0.15	30	http://www.highlandeco.com/
17	T	Grytviken	Grytviken	South Georgia	0.472	65	https://www.gilkes.com/
18	T	Pungwe B	Honde Valley	Zimbawe	3	176	https://www.gilkes.com/
19	V	Isola Dovarese HPP	Isola Dovarese	Italy	11.75	3.2	http://www.vlh-turbine.com/
20	U	Queen's Mill	Castelford	UK	3.9	2.1	Quaranta (2020)
21	U	Undershot Waterwheel	-	-	0.28	0.58	Quaranta (2020)
22	U	Treviso Waterwheel	Treviso	Italy	1.38	0.95	Quaranta (2020)
23	O	Hydrowatt	-	-	0.6	3	Quaranta and Revelli (2018)
24	O	Cooperation project MAE-FAO	-	Italy	0.04	5.5	Quaranta and Revelli (2018)
25	O	Alan Stoyel and Graham Hackney	-	-	0.15	3.5	Quaranta (2020)
26	B	Moter Saenger	-	-	0.7	2.6	Quaranta (2020)
27	B	Rigamonti Giovanni	Pusiano	Italy	0.1	1.6	Quaranta (2020)
28	B	The Mill of Borgo Cornalese	Villastellone	Italy	1	1.85	Quaranta and Revelli (2018)

The Widdington site in Linton-on-Ouse, York, United Kingdom hosts the largest Archimedes screw generator in the world (at time of construction in 2017) [45]. Due to its large diameter ($D_o = 5\ m$) it can operate at flow rates of up to nearly $Q = 13.5\ \mathrm{m}^3/\mathrm{s}$ to produce a nominal power of about 280 kW. The smallest-scale Archimedes screw known to be installed for energy generation is the *PicoPica10* device manufactured by Sumino Co., Ltd. (Ena City, Japan). It is a modular screw generator that can produce up to 10 W of electrical energy; the same scale as some laboratory experiments in the ASG literature [46,47]. The company also produces a 500 W variant. Consequently, the Archimedes screw may be implemented as a pico-hydro, micro-hydro, or mini-hydro device effectively. The operating range of Archimedes screws make the device suitable for off-grid, rural installations. The simple, robust design of ASGs also make them candidates for on-site or localised manufacturing; Archimedes screws have been manufactured since antiquity as pumps and the design has not significantly changed. However, the optimization of ASG design for this wide range of operating conditions requires an accurate performance-predicting model.

There are a few performance models in the literature that predict power production and various power losses associated with ASG operation [2,48–52]. However, the models are mostly developed with data from laboratory-scale installations and are not robustly tested against data from the entire operating range of ASGs. Laboratory-scale experiments and data are documented in the literature [46,47,58–67,49,68,50,51,53–57]. The literature also includes some assessments of full-scale ASGs [2,15,69–72], but most lack sufficient instrumentation or documentation to make using their findings feasible for model evaluation.

To resolve the lack of full-scale ASG performance data, the authors and their research partner were planning to fully instrument new, planned installations in Canada. However, due to recent changes in the political landscape, installing these Archimedes screw plants in a timely manner was no longer an

option. A survey and measurement campaign was then planned to gather some data from various installations in the United Kingdom, where more than 60 ASGs are currently operating [13].

There are many more ASGs in several other European countries. The common (English) language shared between the researchers and ASG operators was an important factor in the UK focus of this study. This language commonality simplified establishing connections with plant operators to arrange plant access, and in practice allowed much more detailed discussion of observations and technical issues than would not have been possible without a shared language. Much of the significant work on Archimedes screw generators and pumps has been reported in non-English literature, particularly in German and Dutch. The authors do not have fluency in these languages, and have experienced first-hand the difficulty of determining detailed technical information from literature in other languages, even when those languages are relatively similar (i.e., English, German, and Dutch share similar structure and vocabulary). The authors are aware of some Archimedes screw work in Japan, and have reason to believe ASGs have also been studied in China but the significant language differences in these cases have prevented truly thorough searches for this literature.

2. Methods

The research team conducted two trips to the United Kingdom to gather full-scale ASG performance data. The first trip involved site visits to the powerplants shown in Table 2, while the second trip focussed on three powerplants (Table 3). These two trips will be outlined in this section.

2.1. Preliminary Surveying Trip

The first trip occurred in April 2019 to survey and measure datum points throughout a series of power plants, measure screw dimensions as per Fig. 3, and collect power production values as well as operating ranges of flow, head, and rotation speed.

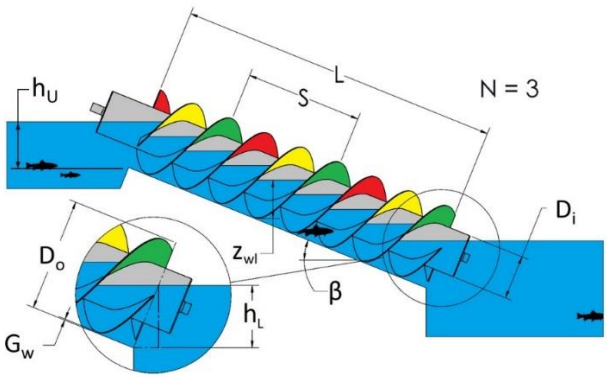

Figure 3: Dimensions of an Archimedes screw [19]**.**

Most of the screw powerplants in the United Kingdom experience highest flow and head in the winter months. The preliminary trip was carried out to identify optimal sites for a more detailed measurement campaign. Site-specific details were documented to help with further detailed measurements and to ensure the right equipment was available. Table 2 shows the sites visited, their locations, and various geometric and design parameters for reference.

160 **Table 2: sites that were visited and surveyed on the first trip of the measurement campaign (1 of 3).**

Site		Linton		Widdington		Goldsborough		Howsham Mill (1)	
Town		Linton-on-Ouse		Linton-on-Ouse		Knaresborough		Howsham	
Region		York		York		York		York	
Year Installed		2012		2017		2014		2007	
Approximate Coordinates		54°02′01.4″N 1°14′17.8″W		54°02′01.4″N 1°14′17.8″W		53°59'51.6"N 1°26'28.5"W		54°03'21.4"N 0°53'09.7"W	
Screw Dimensions	D_o	3	m	5	m	-	m	-	m
	D_i	-	m	2.22	m	-	m	-	m
	L	8.5	m	7.5	m	-	m	-	m
	S	-	m	5.0625	m	-	m	-	m
	N	4	-	4	-	4	-	-	-
	β	22	°	22	°	22	°	-	°
Rated/Expected Levels	Q	4.5	m^3/s	14.5	m^3/s	-	m^3/s	-	m^3/s
	ΔH	3.2	m	3	m	2	m	-	m
	P	101	kW	355	kW	100	kW	24	kW
Photograph				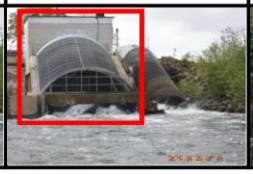					

161

162 **Table 2 (continued): sites that were visited and surveyed on the first trip of the measurement campaign (2 of 3).**

Site		Howsham Mill (2)		New Mills / Torrs Hydro		Church Minshull		River Dart Country Park	
Town		Howsham		New Mills		Church Minshull		Ashburton	
Region		York		Derbyshire		Cheshire		Devon	
Year Installed		2017		2008		2018		2008	
Approximate Coordinates		54°03'21.4"N 0°53'09.7"W		53°22'01.2"N 2°00'25.2"W		53°08'37.6"N 2°29'51.7"W		50°31'02.7"N 3°47'20.6"W	
Screw Dimensions	D_o	-	m	2.6	m	-	m	2.24	m
	D_i	-	m	1.22	m	-	m	1.12	m
	L	-	m	9	m	-	m	11.54	m
	S	-	m	-	m	-	m	2.308	m
	N	-	-	-	-	-	-	3	-
	β	-	°	22	°	Variable	°	22	°
Rated/Expected Levels	Q	-	m^3/s	-	m^3/s	-	m^3/s	-	m^3/s
	ΔH	-	m	3	m	-	m	4	m
	P	55	kW	63	kW	80	kW	65	kW
Photograph									

163

Table 2 (continued): sites that were visited and surveyed on the first trip of the measurement campaign (3 of 3).

Site		Buckfast Abbey		Totnes		Tipton		Windsor / Romney Weir	
Town		Buckfastleigh		Totnes		Lancercombe		Windsor	
Region		Devon		Devon		East Devon		Berkshire	
Year Installed		2012		2015		2010		2013	
Approximate Coordinates		50°29'33.2"N 3°46'31.3"W		50°26'19.2"N 3°41'24.2"W		50°43'29.4"N 3°17'16.8"W		51°29'17.2"N 0°36'22.0"W	
Screw Dimensions	D_o	2.5	m	3.7	m	2	m	4	m
	D_i	1.22	m	1.62	m	0.914	m	1.6	m
	L	10.562	m	9.1	m	7.261	m	5.85	m
	S	2.5	m	3.71	m	2.34	m	4	m
	N	4	-	4	-	3	-	5	-
	β	26	°	22	°	22	°	6 to 20	°
Rated/Expected Levels	Q	-	m^3/s	2 x 6.5	m^3/s	1.5	m^3/s	2 x 10.4	m^3/s
	ΔH	-	m	3.45	m	2.6	m	2	m
	P	84	kW	2 x 160	kW	28	kW	2 x 157	kW
Photograph									

Relative heights of water surfaces and plant components were measured using conventional surveying techniques. Two individuals were necessary for these measurements: one to operate a manual transit, and the other to place and hold-steady a survey pole at desired locations throughout the plant. Desired locations typically included a point on the inlet and outlet of the screw, a point of the screw frame, and the location of gates and other fixed items at the installation (i.e. sluice gate, generator, grid-connection, etc.). Once the site survey was carried out, the water levels at the plant were measured to compare and recalibrate on-site sensors. The site was then well documented with written notes, photography, and videography.

Notes were taken about screw performance, maintenance, operating issues, and various other site-specific details. Photography was used to document the locations of each measurement and to document various design aspects of the plants. Video footage was used to measure the rotation speed of the screw, document screw filling and to capture the wave-action exhibited in the screw buckets as they translate along the length of the screw.

A Sontek FlowTracker2 handheld Acoustic Doppler Velocimeter (ADV®) (Sontek, San Diego, USA) was made available during the surveying trip in case water velocity could be measured freely, but it was found that measuring velocity and flow rate would require further access from site owners and operators. (Access was granted for the next trip during the high flow season.)

Flow rate of water in channels is difficult to measure with low uncertainty, and in these studies the on-site flow rate measurements were the most difficult to gather accurately. Most sensors, like the Sontek ADV® sensor, measure velocity at a point. Both the longitudinal bedform and cross-sectional area of the inlet channel affect overall channel flow rate. A long, straight channel will exhibit predictable near-uniform flow rates for given water levels. However, on the other extreme, a short channel with a sharp bend will be more visibly subjected to minor losses and flow regime changes.

A range of velocity measurements were required at points across a cross-sectional mesh to determine the overall volume flow rate of water through the screw. If these measurements were taken in a long, straight channel then a rating curve could be developed to compare water depth (or stage) to the flow rate (or discharge) in the channel. Afterwards, the measurements were spatially integrated to determine the flow rate. There was a trade-off between grid resolution and accuracy during the flow measurements: a finer mesh yielded more accurate results but required significantly more time to measure. Measuring time played a roll in the error, however, since the flow rate commonly changed as time passed; biasing the flow measurement.

Altogether, accurate flow measurements were required to be taken as quickly as possible along the cross-section of a long, straight inlet channel for the results to be acceptable to any degree of accuracy. During the surveying trip, sites were identified that would make viable candidates for flow rate measurements. These sites included: River Dart, Buckfast Abby, and Tipton.

2.2. Flow Rate and Performance Measurement Trip

Due to availability and further contact with another site owner, the flow rate and performance measurement trip was planned for February 2020 with visits to Buckfast Abbey and an installation owned and operated by a community hydro group, Whitby Esk Energy, in Ruswarp, North Yorkshire. A follow-up visit was also planned for the installation in Totnes due to the regular and significant variation in outlet water level caused by tidal variation at the screw outlet. Table 3 indicates the sites visited, their locations, and their geometric and design parameters.

Table 3: sites that were visited during the flow and performance measurement trip.

Site		Ruswarp		Buckfast Abbey		Totnes	
Town		Ruswarp		Buckfastleigh		Totnes	
Region		North Yorshire		Devon		Devon	
Approximate Coordinates		54°28'05.5"N 0°38'01.1"W		50°29'33.2"N 3°46'31.3"W		50°26'19.2"N 3°41'24.2"W	
Screw Dimensions	D_o	2.9	m	2.5	m	3.7	m
	D_i	1.2	m	1.22	m	1.62	m
	L	5.1167	m	10.562	m	9.1	m
	S	3.07	m	2.5	m	3.71	m
	N	3	-	4	-	4	-
	β	22	°	26	°	22	°
Exhibited Levels	Q	3.95	m^3/s	2.33	m^3/s	-	m^3/s
	ΔH	0.963	m	4.33	m	-	m
	P	27.8	kW	74.3	kW	329.2 (total)	kW
Photograph							

The measurement goals and methods for each of these site visits will be discussed in further detail within this section.

2.2.1. Ruswarp Hydro

Preparations and planning for the Ruswarp Hydro site visit were carried out via email communication with the community hydro group, Esk Energy (Yorkshire). Since this site had yet been visited in-person, the same surveying equipment from the first trip was brought and used to confirm elevations reported in construction drawings provided by Esk Energy. Fig. 4 illustrates the order and

locations of the measurements taken at Ruswarp overlaid on an overhead view powerplant drawing. Drawings of the Ruswarp installation are shown in the appendix.

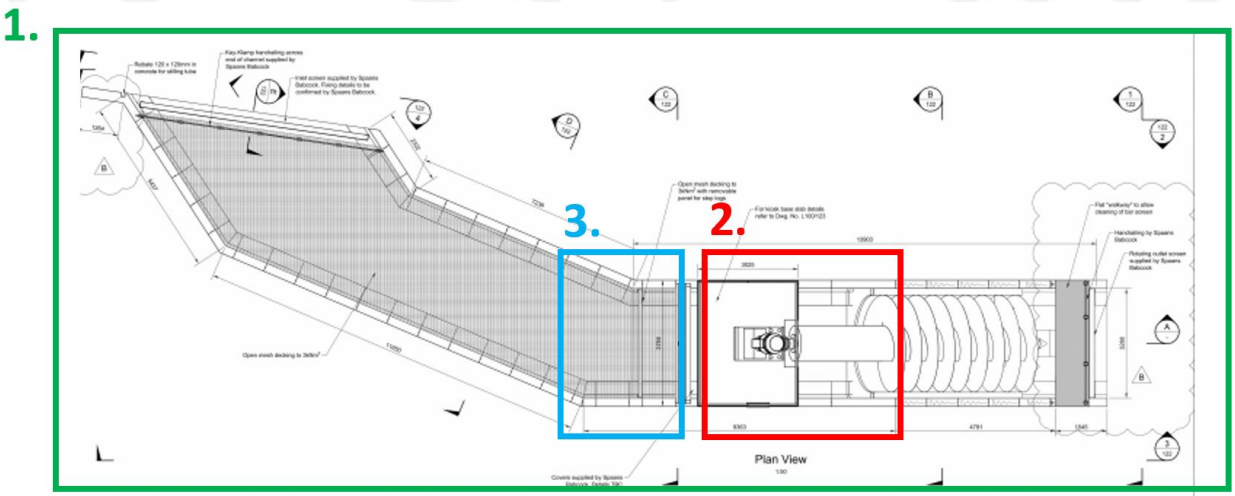

Figure 4: Ruswarp Hydro measurement campaign started with a site survey (1), then measurements within the forebay (2), and finally flow measurements in the inlet channel upstream of the forebay's sluice gate (3).

After a tour of the site, the manual transit was placed between the inlet channel and the fish pass to measure heights of points along the inlet channel, screw frame, and the outlet (Fig. 5). Water levels were measured, and photos were taken at each measurement location for reference. A video was taken of the screw during operation to verify rotation speed and conditions within the bucket. An acoustic range finder sensor was installed on the screw to gather a measurement of the bucket fill height during operation; however, the sensor failed during operation, so these measurements were not recorded.

Figure 5: view of the transit and survey pole. One individual operated the transit while the other steady the survey pole to record a measurement.

The water levels and data points measured with the transit and survey pole were used to verify water levels, re-calibrate sensors, and as a reference point so that site-recorded data could be used to gather further measurements.

Next, the forebay sluice gate was closed, and the screw was drained so that measurements could be taken of the screw and the plant for reference (Fig. 6). These measurements were used to verify screw dimensions and to add a reference point for upper water level (forebay water level) measurements. Future measurements may be made with the monitor camera shown in Fig. 6b. It is interesting to note that the screw was originally designed at a higher point along the weir, however after a design review the screw was shortened. The trough was not shortened until after commissioning when it was found that it contributed to high levels of turbulence at the screw's inlet. The shortening of these components is evidenced by the seam on the inner cylinder and the longer baffle on the upper right side of the trough in Fig. 6a. During operation, the screw exhibited larger levels of overflow due to the shortening and lower position along the weir.

Figure 6: measurements were taken inside the screw's forebay for reference with upper water level measurements. Note in the left image (a) that the baffle on the upper right side of the trough extends past the screw. The right image (b) demonstrates monitor camera placement for tracking inlet water level and bucket filling.

Placement of the top end of the screw on the weir is critical to screw performance. If the screw is placed too low, upper water levels will be too high and cause flooding to the first buckets of the screw. In the event this happens, operators are forced to lower the sluice gate at the inlet to let less water in –

reducing overall plant efficiency. If the screw inlet is placed to high along the weir the initial bucket will be starved during its filling operation and the plant will perform with lower efficiencies due to under-filling.

Finally, the flow measurements were carried out at the site. Point source velocity was measured with the Sontek ADV® sensor along a grid at the cross-section of inlet channel just upstream of the forebay's sluice gate (shown in Fig. 7). A tape measure was placed along the channel cross-section at this location so that the x-position of the measurements could be maintained and documented (Fig. 7b). The Sontek ADV® sensor was equipped with an adjustable pole that was used to measure and control the y-position of the sensor (Fig. 7c). Velocity measurements were taken at 13 horizontal and 7 vertical positions across the inlet cross section (cf. Fig. 13) to characterize the velocity profile. With the location of the velocity measurement on the grid known, the velocity was recorded and integrated spatially to determine the flow rate of the inlet channel. Plant settings were adjusted so multiple flow rates could be measured.

Figure 7: view of sluice gate and flow measurement area from the upstream opening of the inlet channel (left, a), measuring tape placed along the inlet channel's cross-section to measure velocity and known horizontal locations (middle, b), and two individuals with the Sontek ADV® sensor and extended pole ready to measure flow velocity through an open inlet channel grate (right, c).

Due to the bend in the channel, one side of the channel had a very high current, while the other side of the channel had a near stall point. It was very difficult to hold the Sontek ADV® sensor in place due to the rushing water, so the sensor pole was redesigned for the measurements at Buckfast Abbey.

2.2.2. *Buckfast Abbey*

Similar methods were applied to measure flow rate at Buckfast Abbey. Upon arrival at the site, the inlet channel (or mill leat) was examined to select the best location to measure a velocity grid. A birds-eye satellite image of the site is shown in Fig. 8 with the screw installation, inlet channel, and flow measurement locations highlighted. Drawings of the Buckfast Abbey installation are shown in the appendix.

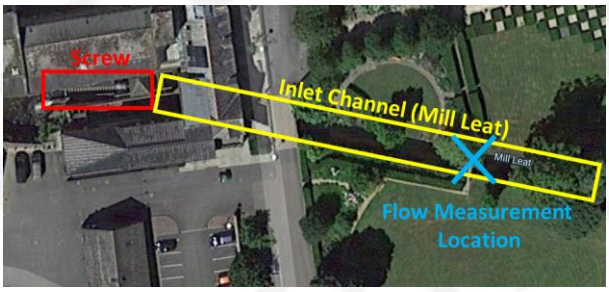

Figure 8: satellite view of Buckfast Abbey site showing screw (red), inlet channel (yellow), and flow measurement (blue) locations.

Upon arrival at the site, the sluice gate at the top end of the inlet channel was set to an 80% opening, allowing the full rated flow to pass through the inlet channel. Velocity was measured across a grid along the cross-section of the channel identified in Fig. 8. It was measured at 15 equally spaced horizontal locations and 4 heights along the cross section spanning from 65 to 460 cm and 0 to 145 cm, respectively. It is noted that the channel cross-section was a small-angled trapezoid and that there was significant debris build-up along the channel bed and walls – which noticeably impacted near-wall velocities (Fig. 9).

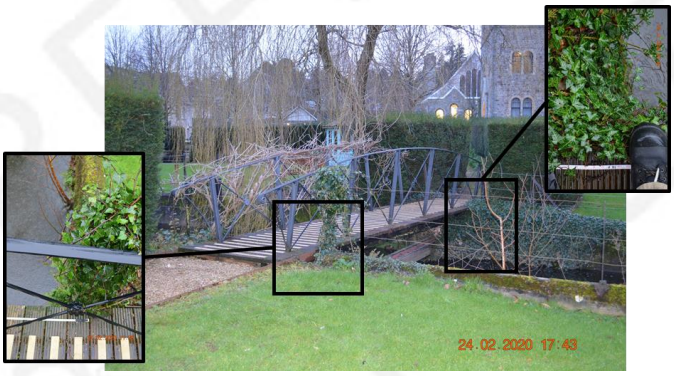

Figure 9: debris on channel side walls affected near-wall velocities.

After the full grid was measured for an 80% sluice gate opening, the gate was set to a 70% opening. The site-recorded water level measurements were plotted in real-time to evaluate when the plant began to operate at equilibrium under the new inlet conditions – it usually took 35 minutes for the plant to "settle" under the new flow rate. Once equilibrium was met, 3 points were measured in the free-stream region of the flow measurement location's cross-section. Since the inlet channel was sufficiently long and straight, the three freestream measurements were used to scale the other measurements of the grid from the initial velocity measurements along the grid (i.e. the 80% sluice gate opening measurements), saving measurement time while still capturing a relatively accurate flow rate reading. This was repeated for a total of 6 different flow rates corresponding to 6 different sluice gate opening values.

It was noted that the outlet water level varied significantly throughout the tests. At the start of the test, the water level was near 80% submersion of the bottom end of the screw (Fig. 10a). Upon completion of the flow measurements the outlet water level was much higher than 120% outlet submersion (Fig. 10b).

Figure 10: outlet water level near the start of measuring (left, a) and at the end of testing (right, b).

This variation in outlet water level had no impact on the flow measurements, but it did lead to a decrease in plant performance since the overall head drop decreased. Practically, measurements of varying outlet water level are very difficult to measure at full-scale installations since water levels are usually steady throughout a single day. While southern England does house very "flashy" watersheds, it

was quite lucky that measurements were able to be gathered with large outlet water level variation throughout a single day since it will help to more robustly evaluate model performance. Only plants with tidal variations at their outlet commonly experience drastic outlet water level variation throughout a day – this is the reason that a follow-up visit was scheduled at the Totnes power plant.

2.2.3. Totnes

The power plant in Totnes houses twin parallel screws that experience tidal variations in their outlet water level. The power plant is shown in a satellite view in Fig. 11. Drawings of the Totnes installation are shown in the appendix.

Figure 11: Totnes power plant has a short inlet and significant outlet water level variation due to impacts of ocean tides. North is upward. The plant is at lower right on the south end of the weir. Flow is from left to right.

During the site visit at Totnes, the inlet channel had large debris build-up which precluded a survey using the flow meter to measure the volume flow rate at the inlet. The inlet of this plant is quite large, and it would have been difficult to conduct an inlet survey even in optimal conditions without debris present. Instead, data was gathered from the on-site computer terminal that recorded power readings for both screws, and the up- and downstream water levels. Data was collected manually for the a few hours of the tidal cycle – enough to see it level-off (Fig. 12). This data was stored for post processing later.

Figure 12: outlet water level near site arrival time (left, a) and at the end of the tidal cycle (right, b).

Visually, the outlet of the screw was about 90% submerged upon arrival, and only about 60% submerged at the end of the tidal cycle. The bankside screw (the nearest screw in Fig. 12) had a recent flighting failure and was operating with $N = 3$ blades rather than $N = 4$. The riverside screw (the further screw in Fig. 12) was operating with all four blades, as designed. The authors noted that the power production of the two screws was nearly identical, with the bankside screw only producing an average of about 3.2% less power. This indicates that the simple, robust design of the screw can operate effectively when experiencing severe failure.

3. Results and Discussion

First, some general observations will be presented from both the surveying trip and the flow and performance measuring trips. Afterwards, results will be presented in a similar order to the methods section starting with Ruswarp Hydro, then Buckfast Abbey and Totnes. Finally, Section 3.5. shows some preliminary results for a follow-up scaling study that will use a computational fluid dynamics (CFD) model evaluated for accuracy against this full-scale data.

3.1. General Archimedes screw plant observations

Eleven Archimedes screw sites were visited in total in the United Kingdom during two trips. It was noted that most of the sites had inclination angles of $\beta = 22°$, with the exception being Buckfast Abbey, Church Minshull, and the Romney Weir. Buckfast Abbey was an exceptionally long screw since it

operated at a relatively high head (nominal $H = 4.2\ m$) location that had historically powered a waterwheel. As such, it was installed at a steeper inclination angle ($\beta = 26\ °$) to allow for a shorter length to reduce capital costs. The installations at Church Minshull and the Romney Weir had variable inclination angles. The plant operator had found highest efficiencies occurred at $\beta = 22°$ for the Romney Weir installation [73].

Most Archimedes screws were designed with $N = 4$ blades, the exceptions being the River Dart Country Park ($N = 3$), Ruswarp Hydro ($N = 3$), and the Romney Weir ($N = 5$). However, after follow-up discussions with the builder, it was suggested that the Romney Weir would likely have produced more power if it were designed with $N = 4$ flights [73]. It is also relevant to note that the $N = 3$ bladed plant at the River Dart Country Park was the first screw plant installed in the UK and likely served as a proof-of-concept.

Aside from the installations at Tipton and Buckfast Abbey, all the screws visited operated with variable speed. Tipton operated with a single speed induction generator to have a lower cost of operation and more efficient mechanical-electrical energy conversion.

Many sites had low average flow rates but very high flood levels. The UK has very "flashy" water systems and are prone to large variation in flow and water levels. It was common to find that even variable-speed screw plants did not operate for long during low flow periods. Without variable-speed controls, many plants would not run most of the time. Two plants (Linton and Church Minshull) had water-proofed generators, and six plants had water-proofed generator rooms or enclosures (Widdington, Goldsborough, Howsham Mill, Totnes, and Romney Weir). Though it was water-proofed, the Totnes installation had fewer flooding concerns; as did the installations at The River Dart and Buckfast Abbey, due to site topography. Ruswarp Hydro installed all flood-sensitive equipment $0.5\ m$ above the 100-year flood level provided by the UK's Environment Agency.

3.2. Ruswarp Hydro

The velocity cross-sectional grid was spatially integrated to find the flow rate for each of the three settings carried out at Ruswarp Hydro. The measurement locations and observed velocities are shown in Fig. 13.

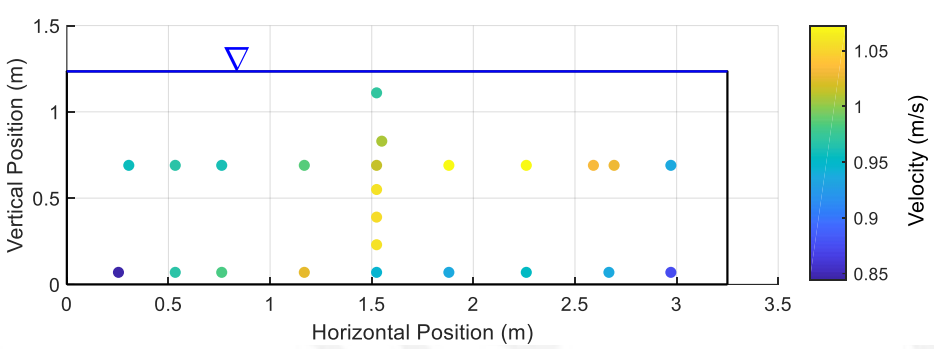

Figure 13: velocity profile along the channel's rectangular cross-section for the first test. The free surface is shown along the top with a blue line. The horizontal channel bed and vertical side walls are shown as black lines. The horizontal position is measured from the south bank of the inlet channel and the vertical position is measured from the channel bed.

The power plant's water levels (upper h_U, lower h_L, and overall head ΔH), measured flow rate (Q), generating torque (T), rotation speed (Ω), mechanical power produced by the screw (P_s), and the electrical power produced by the plant (P_e) are shown in Table 4.

Table 4: Results of the measurements taken at the Ruswarp Hydro ASG plant on 22 February 2020.

Test Number	ΔH (m)	h_U (m)	h_L (m)	Q (m^3/s)	T (Nm)	Ω (RPM)	P_s (kW)	P_e (kW)
1	0.963	1.234	2.030	3.949	11620	26.7	32.5	27.8
2	0.771	1.044	2.054	2.850	12693	20.0	26.6	22.3
3	0.768	0.826	1.878	1.770	14544	18.4	28.0	23.8

Based on the resolution of the velocity grid and the care taken during the measurements, the authors have confidence in the flow measurement of test number 1. However, due to time constraints it was not possible to measure tests 2 and 3 with the same resolution, and the authors are not certain of their validity. Due to the site's complex channel geometry, a higher resolution sample grid was required to make accurate flow measurements. So, the authors caution that data points 2 and 3 have a high degree of uncertainty and might not be as appropriate for model evaluation.

With the torque and rotation speed known, the mechanical power at the shaft was calculated. The mechanical power value (P_s) represent the mechanical conversion capabilities of the Archimedes screw (i.e. its ability to convert hydraulic power into mechanical power for electrical generation). With the water levels, power, and flow rates known, this full-scale dataset may be used to evaluate existing models from the literature, and aide in future model improvements.

3.3. Buckfast Abbey

The results of the measurements taken at Buckfast Abbey are presented in this section. Firstly, the velocity profile at the cross-section of channel where the flow measurements were taken is shown in Fig. 14.

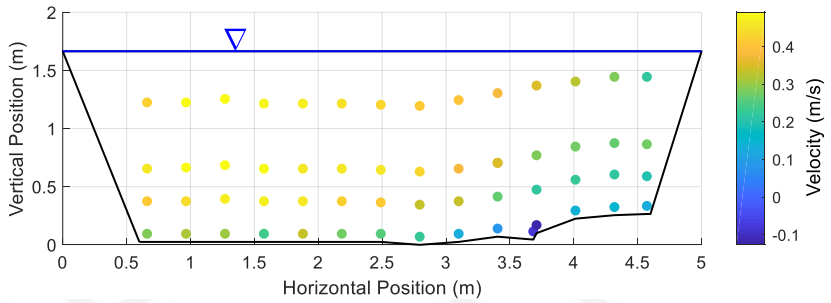

Figure 14: velocity profile along the channel cross-section for the 80% open sluice gate case. The free surface is shown along the top with a blue line. The horizontal channel bed and vertical side walls are shown as black lines. The horizontal position is measured from the south bank of the inlet channel and the vertical position is measured from the channel bed.

As mentioned in Section 2.2.2. the debris on the side walls changed the velocity profile. The change in vertical position is due to variation in the height of the channel bed caused by debris buildup. The velocity profile indicates that the right side of the channel (i.e. 460 cm) had more debris than the left side (i.e. 50 cm). It also indicates that the debris on the channel bed on the bottom right side has a higher roughness height than the left side, since the velocity change was more drastic.

A total of six flow settings were measured during the campaign at Buckfast Abbey. As mentioned previously, the first flow setting had its entire cross-sectional grid measured to develop the velocity profile shown in Fig. 14. Subsequent flow settings were measured at three points along the free-stream

region of the grid, and the velocity profile of Fig. 14 was scaled based on these three points to approximate the curves for all other flow rates. The results of integration along the velocity profile shown in Fig. 14, and the integration of each scaled velocity profile are shown in Table 5.

Table 5: Results of the measurements taken at the Buckfast Abbey ASG plant on 24 February 2020.

Test Number	ΔH (m)	h_u (m)	h_L (m)	Q (m^3/s)	T (Nm)	Ω (RPM)	P_s (kW)	P_e (kW)
1	4.333	1.708	1.978	2.326	27564	28.8	83.0	74.3
2	4.076	1.735	2.261	2.340	25917	28.8	78.1	69.8
3	3.726	1.616	2.492	2.118	20800	28.8	62.7	55.7
4	3.374	1.391	2.620	1.618	12601	28.8	38.0	32.7
5	3.490	1.515	2.628	1.957	16950	28.8	51.1	44.9
6	3.725	1.713	2.591	2.380	22418	28.8	67.5	60.2

The results of Table 5 are shown graphically in Fig. 15, relating the height of water at the point of measurement in the inlet channel to the flow rate in the inlet channel.

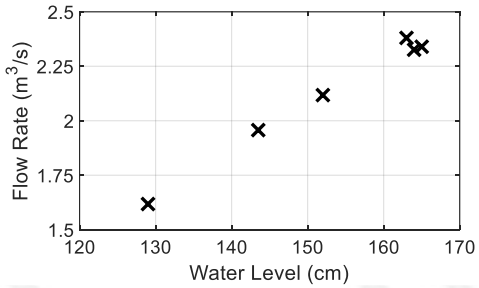

Figure 15: rating curve for Buckfast Abbey inlet channel.

As expected, a predictable trend existed between the water level and the discharge in this long, straight inlet channel. This suggested that future flow rate measurements can be approximated with a measurement of the water level at this location in the channel. Like the Ruswarp measurements, the water levels, flow rates, speed, and power readings of this site were all measured and may thus be used for model development and evaluation.

3.4. Totnes

The final site examined during the second measurement campaign was the screw plant in Totnes. As mentioned, measuring the flow rate was not possible, but the authors did document some interesting data collected from other on-site instrumentation. Figure 16 shows the outlet submergence (ψ_L) and gross plant power production capabilities during six complete tidal cycles. Figure 16a shows ten-second increments of the two measurements, while Figure 16b directly compares the two.

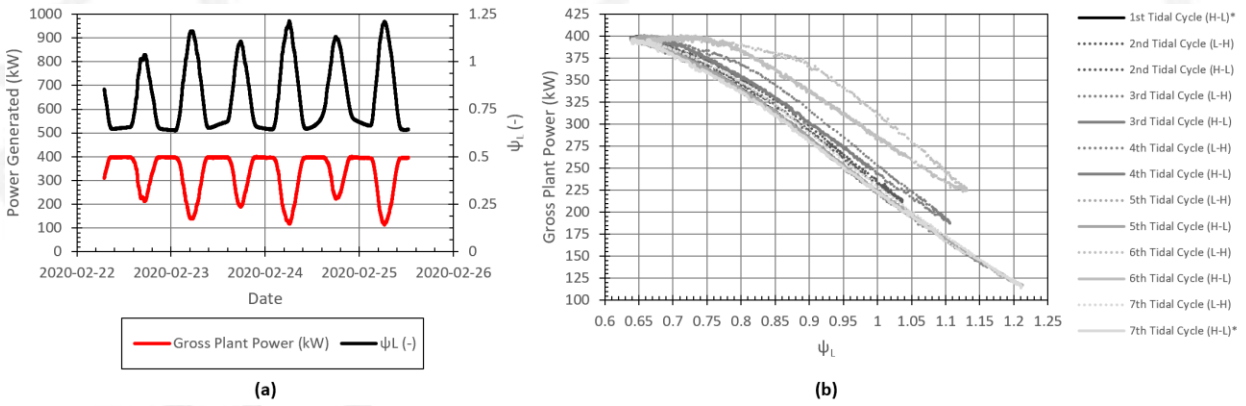

Figure 16: Plot (a) demonstrates the tidal variation effect on plant power production (red) and dimensionless outlet submersion, Ψ_L (black). The same data is directly compared in plot (b).

The authors note that UK guidelines require plants to be designed with an upper limit of power production – in this case, Totnes did not exceed 400 kW of generated power, even if conditions would have allowed greater output. With that in mind, it is apparent that the power output exhibits a dependency on outlet submergence, although apparent hysteresis in Figure 7b indicates the power output is not solely influenced by outlet water level.

The amplitudes varied slightly between the two curves in Figure 17a: the second last “peak” in outlet submergence had a value of $\psi_L \approx 1.13$, and the following “peak” (i.e. the last peak) nearly reached $\psi_L = 1.25$. This is a change of about 110.6%, while the corresponding power production values changed from $P_e \approx 210\ kW$ to $P_e \approx 100\ kW$, meaning a change of about -210%.

Though not enough information was gathered to make this data useful for model development and evaluation, it is still very valuable to directly observe the effect of outlet water level on performance of a full-scale plant.

3.5. Preliminary work evaluating a full-scale CFD model

As in many other fields, there is notable lack of useful measured data in the literature for evaluating the performance of numerical or parametric models of Archimedes screw plants. This lack of evaluation data is one of the most significant limitations on further developing such models, and was the primary motivation for this study.

As an example, the data gathered from the Ruswarp and Buckfast Abbey power plants was used to evaluate a full-scale dynamic CFD model of an Archimedes screw generator plant shown in Fig. 17. The model is discussed in greater detail in the literature [74].

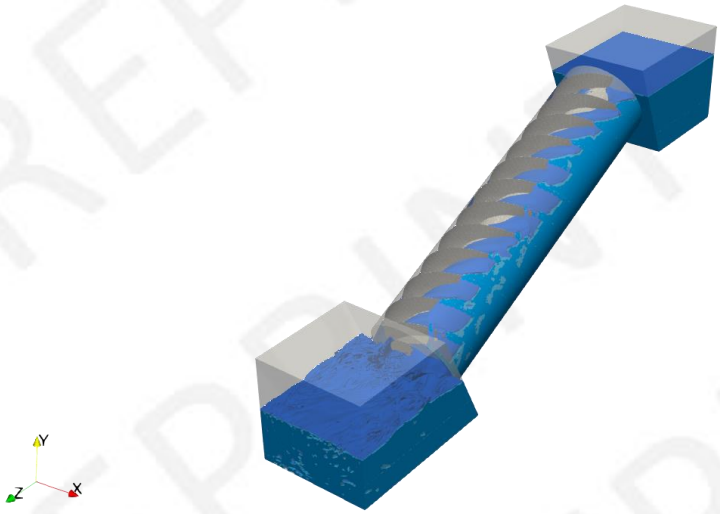

Figure 17: full-scale dynamic CFD model of an ASG power plant.

The flow rate and rotation speed measured on-site were used to set up the model, and the model was run until it converged. The averaged values were then plotted against experimental observations

and measured values in Fig. 18 to evaluate the accuracy of the CFD simulations. The additional data points in Fig. 18 come from laboratory studies [49,50,62,74] and other field studies [50,61,72].

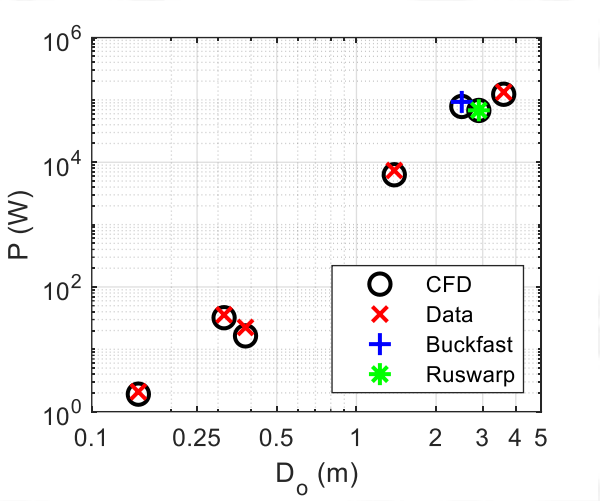

Figure 18: comparison of CFD simulation results to measurements and experimental data. Experimental data gathered from Buckfast Abbey and Ruswarp Hydro are highlighted.

The CFD model successfully predicted screw performance across a wide range of installation sizes. A log-scale plot was needed to show the wide range of the data points; however, it minimized the apparent differences between the simulated and measured values. Differences were minor, but still present. Some of the minor discrepancies between the simulated and measured values may be due to the differences in geometry between the simulated and measured screws. The CFD simulation models a geometrically perfect screw while the real-world screw plants and laboratory screws have imperfections. For example, the gap width of the simulation is perfectly uniform, where a real screw will have some differences across its perimeter within manufacturing tolerances, causing a slightly variable gap width. The CFD simulation domain was scaled across the range, and so differences in the geometry of the delivery channels of the real-world screws were not modelled. For example, both Buckfast and Ruswarp have a smoothed, inlet fairing treatment to reduce hydraulic losses. However, the CFD simulation used the sharp inlet transition between the upper reservoir and trough shown in Fig. 17 and did not match the real-world reservoir geometry.

4. Design Insights

The authors have compiled this section to offer some practical insight based on the site surveys, measurements, and experimentation in this study. It offers some insights and considerations for ASG powerplant design.

4.1. Power production estimates

There is no simple way to accurately approximate screw power; however, Nuernbergk [75] created a table to estimate the screw's optimal mechanical efficiency based on its outer radius and rotation speed. The table shows the mechanical efficiency of Archimedes screws (converting pressure to mechanical torque); ASGs have high mechanical efficiencies, upwards of 80%. ASGs perform with relatively high river-to-wire efficiencies as well; some plants perform with river-to-wire efficiencies higher than 75%. Once the mechanical efficiency was approximated, the optimal shaft power could be estimated by:

$$P_s = \eta P_a = \eta \rho g H Q$$

Full performance prediction models are more complicated. Nuernbergk outlined various power prediction and power loss models in the German-language book Wasserkraftschnecken [75], and Lubitz [49] presented a performance model with subsequent publications to update power loss modelling techniques [50,62,76]. Accuracy improvements are underway using the full-scale powerplant data gathered in this study. Generally, the model used flow rate, upper and lower water levels, rotation speed, and the screw's geometry to estimate power. Functionally, the model calculates the average fill height in the screw's buckets, then integrates along the blades to convert the blade pressure to a torque about the rotational axis. The torque is then multiplied by the average number of buckets in the screw and the rotation speed to find the total power production; more details may be found in the cited literature.

4.2. Inclination angle

It is most common to observe screw generators with inclination angles of $\beta = 22°$, this is also a very common inclination for screw pumps. The Romney Weir installation has a varying inclination angle; the plant owner documented screw performance under varying inclination angles and found the optimal inclination to be approximately $\beta = 22°$. Numerical simulations suggest that the optimum inclination angle is between $\beta = 20°$ to 25°, supporting these claims.

However, the authors suggest that the optimum inclination angle is site-specific, and dependent on other screw geometry variables (e.g. number of blades, etc.). Numerical simulations showed that the simulated screw geometry with N=3 blades performed at its highest efficiency when $\beta \approx 15°$. The same study found the optimal efficiency of a 4- and 5-bladed variant was at $\beta \approx 20°$ and 25°, respectively.

Powerplant design is usually based on return on investment (ROI). Some screws that have higher head drops may be installed at steeper inclinations to lessen the cost of civil works. For example, Buckfast abbey has a proportionally large head drop, which is likely why it was installed with an inclination of $\beta = 26°$, rather than the conventional 22°.

4.3. Diameter ratio

The diameter ratio of screw pumps was theorized to be optimal at $D_o/D_i = 0.54$ [77]. The optimum was found by maximizing the volume within a screw's bucket, so it is applicable to screw generators as well. Archimedes screw generators have commonly been installed with diameter ratios to approximately match the theoretical maximum. Usually, the inner cylinder of the screw is a standard sized pipe, and the blades are built to match the outer diameter requirements. So, in practice, the diameter ratio is a target value.

4.4. Pitch and screw length

In practice, most screws have a pitch-diameter ratio of $S/D_o = 1$. Laboratory-scale experimentation found agreement with this ratio [46]; three screws with $S/D_o = 1.4$, 1.0, and 0.8 were compared, the screw with $S/D_o = 1.0$ produced power most efficiently.

In the same experiment, screws with varying pitch-length ratios. The authors classified the test screws as short ($L/S < 1.5$), medium ($1.5 \leq L/S \leq 3$), or long ($L/S < 3$) and compared performance. On the laboratory-scale, the longest screws performed the best. The authors theorise that the screw buckets have more time to fully form and equilibrate, while the screw has more time to convert pressures into mechanical torque when the screw is longer. However, a longer screw is heavier, more expensive, and experiences more friction loss. So, in practice, real world screws tend to be "medium" length in terms of the above study.

4.5. Number of blades

Most screw generators are installed with 3, 4, or 5 bladed screws. It was shown that theoretically more blades yields higher efficiencies for pumps [77], and the same could probably be suggested for generators. However, the addition of blades adds significant costs to manufacturing and installation. The authors have visited one 2-bladed installation at the Cragside House in Rothbury, UK. It is an exceptionally long screw ($L/S \approx 11$); having less blades would reduce overall costs. Overall, it seems that many screws are installed with 3 or 4 blades, this is likely the balance between performance and cost; ultimately, the goal is to produce power the most economical way.

As mentioned above, in follow-up discussions the builder of the Romney Weir installation reflected that the powerplant would likely produce more power if it had 4 blades (and not 5).

A CFD study tested 3-, 4-, and 5-bladed screws and varying inclination angles. The 4- and 5-bladed screws had very similar efficiencies throughout – they were notably higher efficiencies than the 3-bladed

542 screw. At some inclination angles the 5-bladed screw performed with a slightly higher efficiency; the
543 additional blade was suggested to help minimize leakage losses in the screw, improving performance.
544 The authors suggest that the optimal number of blades is dependent on-site conditions. In some cases,
545 the efficiency increase and cost of additional blades improves ROI, in other cases ROI may be improved
546 by foregoing the slight efficiency increase to save the additional costs.

547 ## 4.6. Multiple screw installations

548 Some powerplants have multiple, parallel screws; depending on site conditions, two or mor smaller
549 screws may perform better, or yield a better ROI than one large screw. For example, sites with
550 proportionally low head and high flow would require a large diameter screw to support the desired flow
551 rate. But, to maintain appropriate D_i/D_o and S/D_o ratios, the screw would need to be very short (which
552 corresponds to low efficiencies). In this case, multiple screws with smaller diameters could be installed
553 to support the higher flow rate. By extension, the smaller diameter screws would be proportionally
554 longer, corresponding to higher efficiencies.

555 Sites with highly variable flow conditions and large seasonal flow variation may perform better with
556 multiple screws as well. Depending on site conditions, it may be advantageous to operate one screw at
557 the year-round baseflow and additional screws as flow rates increase. However, this can sometimes be
558 accomplished using a variable speed system.

559 ## 4.7. Variable speed systems

560 Variable speed ASG installations are very common, it allows the screw to accommodate changing
561 flow and head conditions at the site. Variable speed systems use electronic controls to vary the speed of
562 operation such that the screw operates at the optimal point for the given flow and head conditions. As
563 such, it is more difficult to match grid frequencies. At a high level, the power system has a raw
564 alternating current (AC) power produced by the screw that is not likely to be operating at the grid

565 frequency. The power is then passed through a rectifier, converting it to direct current (DC) and finally
566 passed through an inverter to convert it to AC power that matches the grid frequency. This process has
567 been observed to add electrical power losses up to approximately 10% [78]. Some ASG powerplants
568 have system overrides to improve plant performance; they bypass the inverter-rectifier loop when the
569 screw is operating at its design speed that matches the grid frequency.

570 Conversely, fixed-speed screws commonly use induction generators for mechanical-electrical
571 conversion. Induction generators always operate at grid frequency if the rotation speed is higher than
572 the synchronous speed. Induction generators are common for fixed-speed screws since they have a
573 lower cost of operation and are highly efficient.

574 # 5. Conclusion

575 In the end, this measurement campaign yielded a successful data point for the Ruswarp installation
576 (and two other highly uncertain data points), 6 successful data points for the Buckfast Abbey
577 installation, and some interesting and important insight on the day-to-day operations of an ASG power
578 plant. It was determined that the Ruswarp and Buckfast hydropower schemes operated (on the day of
579 measurement) with river-to-wire efficiencies of about 74.5% and 75.3%, respectively. The measured
580 efficiencies seem to be in line with the efficiency ranges given in the literature [3].

581 This campaign also provided some insight into the effect of outlet water level on screw
582 performance; though that dataset was not complete enough for model evaluation and development
583 purposes. These field studies also provided valuable qualitative information to the research team, both
584 due to assuming the role of plant operator while collecting data, and the opportunities for discussion of
585 a range of aspects of plant performance and other factors in plant operation with the operators of the
586 actual plants. Important new avenues of research were identified that were not apparent “from a
587 distance” in the literature. For example, the research team is now examining the degree of power loss

588 due to increased surface roughness on screw surfaces caused by algae growth and other contamination,
589 after this phenomenon was mentioned by two different operators at different plants.

590 This field study methodology presented in this paper would also be feasible in developing regions.
591 There is an inherent value in evaluating the performance of previously installed energy facilities: both in
592 terms of the qualitative and quantitative insights gained. For example, some of the qualitative
593 information (reported by operators) discussed in this article provided important but previously
594 unrecognised research questions, like the impact of algae on power production.

595 One of the major successes of this measurement campaign was that the measured data was able to
596 demonstrate the accuracy of a CFD model when used in a brief verification study. Altogether, this CFD
597 model may be used to extend the known dataset for full-scale installations since it was a quite involved
598 process to gather data from full-scale installations. As evidenced by this report, it took several weeks
599 worth of work (in surveying, travel, measuring, documenting, and post processing with two people),
600 access to specialized measurement equipment and major expenses (in accommodations, flights, and
601 ground transport) to yield seven reasonably accurate full-scale ASG data points.

602 This study also was able to highlight the practical design of ASG powerplants by demonstrating the
603 most common geometry and parameters for installations. Precedent and proof-of-concept are
604 invaluable for designers and may help further advance design optimization of Archimedes screw
605 generators. The successes demonstrated by the Ruswarp Hydro, Buckfast Abbey, and Totnes Hydro
606 installations indicate that Archimedes screw generators are an eco-friendly, cost-efficient, micro-
607 hydropower option. Well-designed Archimedes screw generator installations may help to grow
608 sustainable energy networks world-wide.

Acknowledgements

The authors gratefully acknowledge the help and support of David Mann and Stuart Moore of Mann Power Hydro Ltd. for granting site access, sharing data, and helping with surveying and measurements. We are also very grateful to Colin Mather, Rory Newman, Stephen Larkin, Dave Moore, and the rest of the team at Whitby Esk Energy, for their help and support with surveying and measurements at Ruswarp Hydro. The assistance of the Buckfast Abbey staff was integral to the measurements taken at Buckfast Abbey's Hydro plant and is greatly appreciated. The authors would also like to thank David Dechambeau of Southeast Power Engineering for his help and support with surveying and measurements of the Romney Weir ASG plant in Windsor, UK.

Aspects of Dr. Lubitz' and Mr. Simmons' work was financially supported by the Natural Sciences and Engineering Research Council (NSERC) Collaborative Research and Development (CRD) program (grant numbers CRDPJ 433740-12 and CRDPJ 513923-17) and Greenbug Energy Inc. (Delhi, ON, Canada). Mr. Simmons work was also financially supported by the Ontario Graduate Scholarship program. The authors would like to thank Murray Lyons and Arash YoosefDoost for feedback and assistance during planning and analysis. The assistance of Tony Bouk and Brian Weber of Greenbug Energy Inc. is also gratefully acknowledged.

References

[1] Karl-August Radlik, "Hydrodynamic screw for energy conversion - uses changes in water supply to regulate energy output," Deutches Patent- und Markenamt 4139134A1, 28 Nov., 1991.

[2] D. Nuernbergk, *Wasserkraftschnecken - Berechnung Und Optimaler Entwurf von Archimedischen Schnecken Als Wasserkraftmaschine (Hydropower Screws - Calculation and Design of Archimedes Screws Used in Hydropower)*, 1st ed.Verlag Moritz Schäfer, Detmold, 2012.

631 [3] A. Lashofer, W. Hawle and B. Pelikan, State of technology and design guidelines for the
632 Archimedes screw turbine, in Hydro 2012 - Innovative Approaches to Global Challenges, 2012,
633 pp. 1–8.

634 [4] S.R. Waters, “Analysing the performance of the Archimedes Screw Turbine within tidal range
635 technologies,” M.Sc. thesis, Lancaster University, Lancaster, UK, 2015.

636 [5] International Energy Agency, “Africa Energy Outlook 2019,” International Energy Agency, Paris,
637 France, Report. Nov. 2019.

638 [6] International Energy Agency, “World Energy Outlook 2009,” International Energy Agency, Paris,
639 France, Report. Nov. 2009.

640 [7] B. Ho-Yan, W.D. Lubitz, C. Ehlers and J. Hertlein, *Field Investigations in Cameroon Towards a*
641 *More Appropriate Design of a Renewable Energy Pico Hydro System for Rural Electrification*, in
642 *Technologies for Sustainable Development*, J. Bolay, S. Hostettler and E. Hazboun, eds., Springer
643 International Publishing, 2014, pp. 43–56.

644 [8] Independent Evaluation Group, *The Welfare Impact of Rural Electrification : A Reassessment of*
645 *the Costs and Benefits*, Vol. 02, The World Band, Washington, 2008.

646 [9] World Health Organization (WHO), “Household air pollution and health,” World Health
647 Organization (WHO), 2018. [Online]. Available at https://www.who.int/news-room/fact-
648 sheets/detail/household-air-pollution-and-health.

649 [10] International Hydropower Association, “Hydropower Status Report,” International Hydropower
650 Association, London, UK, Report. May 2018.

651 [11] Y. Zhou, M. Hejazi, S. Smith, J. Edmonds, H. Li, L. Clarke et al., *A comprehensive view of global*
652 *potential for hydro-generated electricity*, Energy Environ. Sci. 8 (2015), pp. 2622–2633.

[12] M. Lisicki, W. Lubitz and G.W. Taylor, *Optimal design and operation of Archimedes screw turbines using Bayesian optimization*, Appl. Energy 183 (2016), pp. 1404–1417.

[13] A. Lashofer, “Projekt Wasserkraftschnecken Verortung,” *lashofer.at*, 2020. [Online]. Available at https://www.lashofer.at/deutsch/wasserkraftschnecke/projekt-wasserkraftschnecken-verortung/.

[14] O.M. Dada, I.A. Daniyan and O.. Adaranola, *Optimal Design of Micro Hydro Turbine (Archimedes Screw Turbine) in Arinta Waterfall in Ekiti State, Nigeria*, 4 (2014), pp. 34–38.

[15] T. Okamura, R. Kurosaki and M. Takano, *Development and Introduction of a Pico-Hydro System in Southern Tanzania*, Afr. Study Monogr. 36 (2015), pp. 117–137.

[16] J.P.K. Mbay, *Archimède Au Secours de l Électrification Rurale de l’afrique*, OmniScriptum Gmbh, Saarbrücken, 2018.

[17] J. Kenfack, O.V. Bossou, J. Voufo, S. Djom and N. Crettenand, *New Renewable Energy Promotion Approach for Rural Electrification in Cameroon*, in *Renewable Energy in the Service of Mankind Vol II*, A. Sayigh, ed., Springer International Publishing, Geneva, 2016, pp. 429–442.

[18] S.J. Williamson, B.H. Stark and J.D. Booker, *Low head pico hydro turbine selection using a multi-criteria analysis*, Renew. Energy 61 (2014), pp. 43–50.

[19] S.C. Simmons and W.D. Lubitz, *A review of Archimedes screw generators*, Renew. Sustain. Energy Rev. (2020), .

[20] J. Chen, H.X. Yang, C.P. Liu, C.H. Lau and M. Lo, *A novel vertical axis water turbine for power generation from water pipelines*, Energy 54 (2013), pp. 184–193.

[21] J. Chen, W. Lu, Z. Hu, Y. Lei and M. Yang, *Numerical studies on the performance of a drag-type*

vertical axis water turbine for water pipeline, J. Renew. Sustain. Energy 10 (2018), .

[22] A. Ghimire, D.R. Dahal, N. Pokharel, S. Chitrakar, B.S. Thapa and B. Thapa, *Opportunities and Challenges of introducing Francis Turbine in Nepalese Micro Hydropower Projects*, J. Phys. Conf. Ser. 1266 (2019), .

[23] M.M. Uamusse, M. Aljaradin and K.M. Persson, *Micro-Hydropower Plant -Energy Solution Used in Rural Areas, Mozambique*, Sustain. Resour. Manag. J. 2 (2017), pp. 3–9.

[24] C.S. Kaunda, C.Z. Kimambo and T.K. Nielsen, *A technical discussion on microhydropower technology and its turbines*, Renew. Sustain. Energy Rev. 35 (2014), pp. 445–459.

[25] S. Sangal, A. Garg and D. Kumar, *Review of Optimal Selection of Turbines for Hydroelectric Projects*, Rev. Optim. Sel. Turbines Hydroelectr. Proj. 3 (2013), pp. 424–430.

[26] D. Matsushita, R. Moriyama, K. Nakashima, S. Watanabe, K. Okuma and A. Furukawa, *Tentative study on performance of darriues-type hydroturbine operated in small open water channel*, IOP Conf. Ser. Earth Environ. Sci. 22 (2014), pp. 0–10.

[27] A. Kadier, M.S. Kalil, M. Pudukudy, H.A. Hasan, A. Mohamed and A.A. Hamid, *Pico hydropower (PHP) development in Malaysia: Potential, present status, barriers and future perspectives*, Renew. Sustain. Energy Rev. 81 (2018), pp. 2796–2805.

[28] E. McLean and D. Kearney, *An evaluation of seawater pumped hydro storage for regulating the export of renewable energy to the national grid*, Energy Procedia 46 (2014), pp. 152–160.

[29] R. Uhunmwangho, M. Odje and K.E. Okedu, *Comparative analysis of mini hydro turbines for Bumaji Stream, Boki, Cross River State, Nigeria*, Sustain. Energy Technol. Assessments 27 (2018), pp. 102–108.

[30] R. Fraser, C. Deschênes, C. O'Neil and M. Leclerc, *VLH: Development of a new turbine for Very Low Head sites*, Proc. 15th Waterpower 10 (2007), pp. 1–9.

[31] P. Kemp, C. Williams, R. Sasseville and N. Anderson, *Very low head turbine deployment in Canada*, IOP Conf. Ser. Earth Environ. Sci. 22 (2014), .

[32] W. Nuantong and S. Taechajedcadarungsri, *Optimal design of VLH axial hydro-turbine using regression analysis and multi-objective function (GA) optimization methods*, J. Appl. Fluid Mech. 9 (2016), pp. 2291–2298.

[33] J. Razak, Y. Ali and M. Alghoul, *Application of crossflow turbine in off-grid pico hydro renewable energy system*, Recent Adv. Appl. Math. (2010), pp. 519–526.

[34] A.K. Yahya, W.N.W.A. Munim and Z. Othman, *Pico-hydro power generation using dual pelton turbines and single generator*, Proc. 2014 IEEE 8th Int. Power Eng. Optim. Conf. PEOCO 2014 (2014), pp. 579–584.

[35] E. Quaranta, *Stream water wheels as renewable energy supply in flowing water: Theoretical considerations, performance assessment and design recommendations*, Energy Sustain. Dev. 45 (2018), pp. 96–109.

[36] E. Quaranta, *Estimation of the permanent weight load of water wheels for civil engineering and hydropower applications and dataset collection*, Sustain. Energy Technol. Assessments 40 (2020), pp. 1–8.

[37] E. Quaranta and R. Revelli, *Gravity water wheels as a micro hydropower energy source: A review based on historic data, design methods, efficiencies and modern optimizations*, Renew. Sustain. Energy Rev. 97 (2018), pp. 414–427.

[38] MJ2 Technologies S.A.S., "Case Studies: VLH Turbines," *Sorgent.e Capital*, 2018. [Online].

717 Available at www.vlh-turbine.com/documents/%0D.

718 [39] Ossberger Hydro, “Ossberger Hydro Projects,” *ossbergerhydro.com*, 2019. [Online]. Available at
719 http://www.ossbergerhydro.com/projects.html.

720 [40] Voith GmbH & Co. KGaA, “Kaplan turbines,” *voith.com*, 2018. [Online]. Available at
721 http://www.voith.com/ca-en/products-services/hydro-power/turbines/kaplan-turbines-
722 560.html.

723 [41] GE Renewable Energy Division, “Kaplan hydro turbine”, *ge.com*, 2019. [Online]. Available at
724 https://www.ge.com/renewableenergy/hydro-power/large-hydropower-solutions/hydro-
725 turbines/kaplan-turbine.

726 [42] M. Eisenring, *Micro Pelton Turbines*, 1st ed.Swiss Center for Appropriate Technology, St. Gallen,
727 Switzerland, 1991.

728 [43] Gruner AG, “Akköy ll: Giresun, Turkey,” *gruner.ch*, 2019. [Online]. Available at
729 https://www.gruner.ch/en/references/styt-ref-d-akkoey-ll.

730 [44] Gilbert Gilkes & Gordon Ltd., “Case Studies: Our global projects,” *gilkes.com*, 2020. Available at
731 https://www.gilkes.com/case-studies.

732 [45] Landustrie Sneek BV, “Hydropower: Linton Lock (UK),” *landustrie.nl*, 2017. [Online]. Available at
733 https://www.landustrie.nl/en/products/hydropower/projects/linton-lock.html.

734 [46] S. Simmons, K. Songin and W. Lubitz, Experimental investigation of the factors affecting
735 Archimedes screw generator power output, in HYDRO 2017 (7-11 October 2017), 2017.

736 [47] G. Dellinger, S. Simmons, W.D. Lubitz, P.A. Garambois and N. Dellinger, *Effect of slope and*
737 *number of blades on Archimedes screw generator power output*, Renew. Energy (2019), pp. 896–

908.

[48] G. Müller and J. Senior, *Simplified theory of Archimedean screws*, J. Hydraul. Res. 47 (2009), pp. 666–669.

[49] W.D. Lubitz, M. Lyons and S. Simmons, *Performance Model of Archimedes Screw Hydro Turbines with Variable Fill Level*, J. Hydraul. Eng. 140 (2014), pp. 1–11.

[50] A. Kozyn and W.D. Lubitz, *A power loss model for Archimedes screw generators*, Renew. Energy 108 (2017), pp. 260–273.

[51] J. Rohmer, D. Knittel, G. Sturtzer, D. Flieller and J. Renaud, *Modeling and experimental results of an Archimedes screw turbine*, Renew. Energy 94 (2016), pp. 136–146.

[52] D.M. Nuernbergk and C. Rorres, *An Analytical Model for the Water Inflow of an Archimedes Screw Used in Hydropower Generation*, J. Hydraul. Eng. 139 (2012), pp. 120723125453009.

[53] M. Lyons and W.D. Lubitz, Archimedes screws for microhydro power generation, in Proceedings of the ASME 2013 7th International Conference on Energy Sustainability & 11th Fuel Cell Science, 2013, pp. 1–7.

[54] W. Hawle, A. Lashofer and B. Pelikan, Lab Testing of the Archimedean Screw, in Hidroenergia 2012, 2012.

[55] T. Saroinsong, R. Soenoko, S. Wahyudi and M.N. Sasongko, *The effect of head inflow and turbine axis angle towards the three row bladed screw turbine efficiency*, Int. J. Appl. Eng. Res. 10 (2015), pp. 16977–16984.

[56] A. Kozyn and W. Lubitz, *Experimental Validation of Gap Leakage Flow Models in Archimedes Screw Generators*, in *Renewable Energy in the Service of Mankind Vol I*, Sayigh A., ed., Springer

759 International Publishing Switzerland, Cham, 2015, pp. 365–375.

760 [57] G. Dellinger, P. Garambois, M. Dufresne, A. Terfous, J. Vazquez and A. Ghenaim, *Numerical and*
761 *experimental study of an Archimedean Screw Generator*, 28th AHR Symp. Hydraul. Mach. Syst.
762 Grenoble, July 4-8 2 (2016), pp. 1419–1428.

763 [58] T. Saroinsong, R. Soenoko, S. Wahyudi and M.N. Sasongko, *Fluid Flow Phenomenon in a Three-*
764 *Bladed Power-Generating Archimedes Screw Turbine*, J. Eng. Sci. Technol. Rev. 9 (2016), pp. 72–
765 79.

766 [59] Erinofiardi, A. Nuramal, P. Bismantolo, A. Date, A. Akbarzadeh, A.K. Mainil et al., Experimental
767 Study of Screw Turbine Performance based on Different Angle of Inclination, in Energy Procedia,
768 110 (2017), pp. 8–13.

769 [60] K. Anzawa, A. Müller, T. Tanaka and K. Yamaishi, Small Hydro from Fukushima – An Energy
770 Revolution 1 kW at a Time, in HydroVision 2017, 2017.

771 [61] A. Passamonti, “Investigation of energy losses in laboratory and full-scale Archimedes screw
772 generators,” M.Sc. thesis, Politechnico di Milano, Milan, Italy, 2017.

773 [62] K.J. Songin and W.D. Lubitz, *Measurement of fill level and effects of overflow in power-generating*
774 *Archimedes screws*, J. Hydraul. Res. 57 (2018), pp. 635–646.

775 [63] J.L. Straalsund, S.F. Harding, D.M. Nuernbergk and C. Rorres, *Experimental evaluation of*
776 *advanced Archimedes hydrodynamic screw geometries*, J. Hydraul. Eng. 144 (2018), pp. 1–10.

777 [64] A. Khan, S. Simmons, M. Lyons and W. Lubitz, Inlet Channel Effects on Archimedes Screw
778 Generators, in Proceedings of The Canadian Society for Mechanical Engineering International
779 Congress 2018, 2018.

[65] R. Dhakal, S. Dhakal, N. Koirala, S.C. Itani, S. Bhandari, G.B. Amgain et al., *Prospects of off Grid Energy Generation through Low Head Screw Turbine in Nepal*, 7th Int. IEEE Conf. Renew. Energy Res. Appl. ICRERA 2018 (2018), pp. 537–543.

[66] G. Dellinger, S. Simmons, W.D. Lubitz, P.-A. Garambois and N. Dellinger, *Effect of slope and number of blades on Archimedes screw generator power output*, Renew. Energy (2018), .

[67] A.I. Siswantara, Warjito, Budiarso, R. Harmadi, M.H. Gumelar and D. Adanta, *Investigation of the α angle's effect on the performance of an Archimedes turbine*, Energy Procedia 156 (2019), pp. 458–462.

[68] S. Simmons, G. Dellinger, M. Lyons, A. Terfous, A. Ghenaim and W.D. Lubitz, *The effects of inclination angle on Archimedes screw generator power production with constant head*, J. Hydraul. Res. (2020), .

[69] K. Brada, *Wasserkraftschnecke ermöglicht Stromerzeugung über Kleinkraftwerke [Hydraulic screw generates electricity from micro hydropower stations]*, Maschinenmarkt Würzbg. (1999), pp. 52–56.

[70] N. Fergnani and P. Silva, Energetic and economic assessment of an Archimedean screw with variable speed operation under variable flows, in HYDRO 2015, 2015.

[71] N. Fergnani and P. Silva, *Technical and economic assessment of an Archimedean screw with variable speed operation under variable flows*, Milan, 2016.

[72] N. Fergnani, P. Silva and D. Bavera, Efficiency assessment of a commercial size Archimedean screw turbine based on experimental data, in Hydro 2017, 2017.

[73] *Personal Communication with David Dechambeau*. Southeast Power Engineering Ltd, Windsor, England, 2019.

802 [74] S. Simmons, G. Dellinger, M. Lyons, A. Terfous, A. Ghenaim and W.D. Lubitz, *Effects of Inclination*
803 *Angle on Archimedes Screw Generator Power Production with Constant Head*, J. Hydraul. Eng. 147
804 (2021), pp. 1–12.

805

806 # Appendix

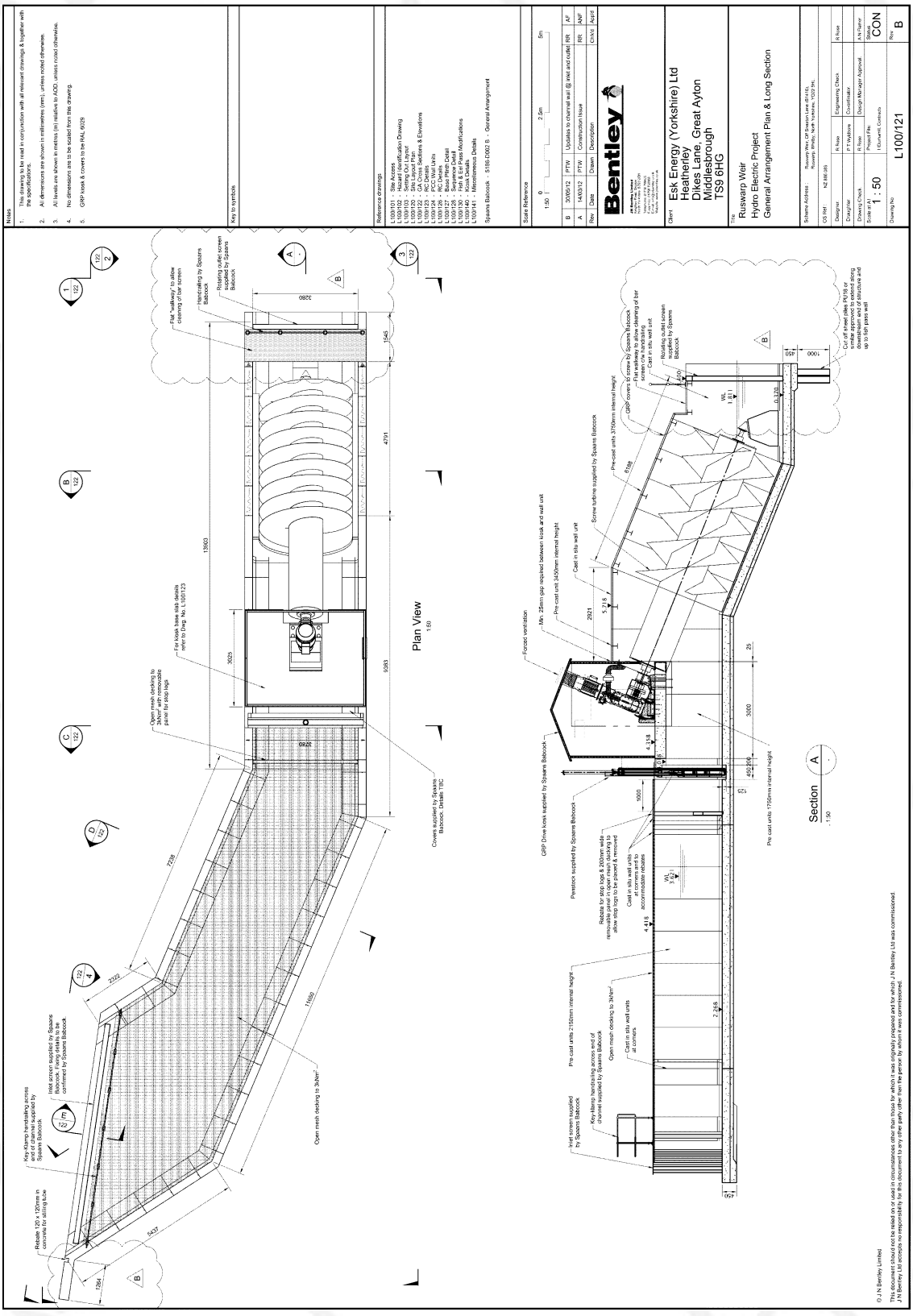

807

Figure A 1: drawing of Ruswarp Hydro installation

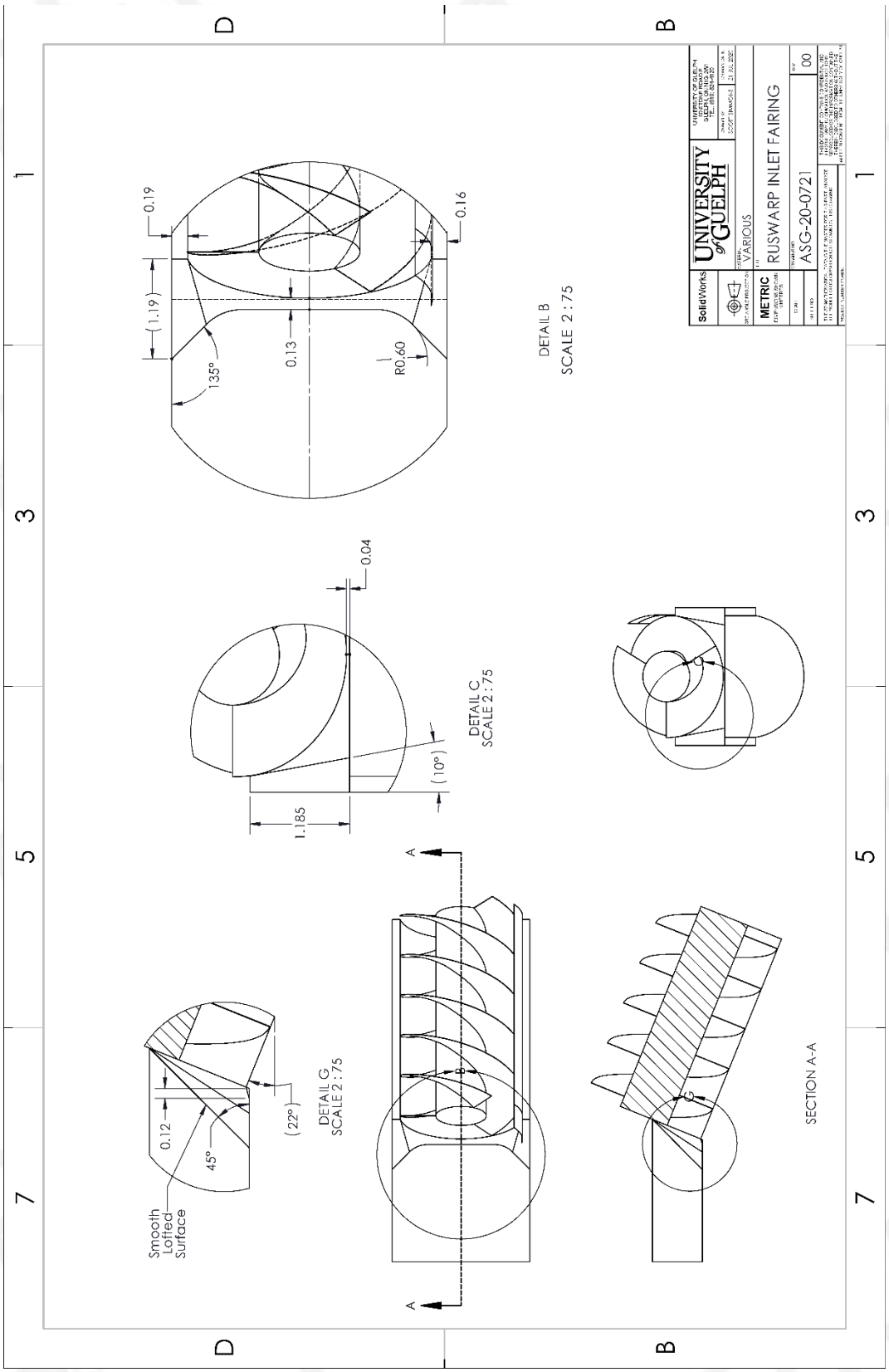

Figure A 2: Ruswarp Hydro forebay measurements.

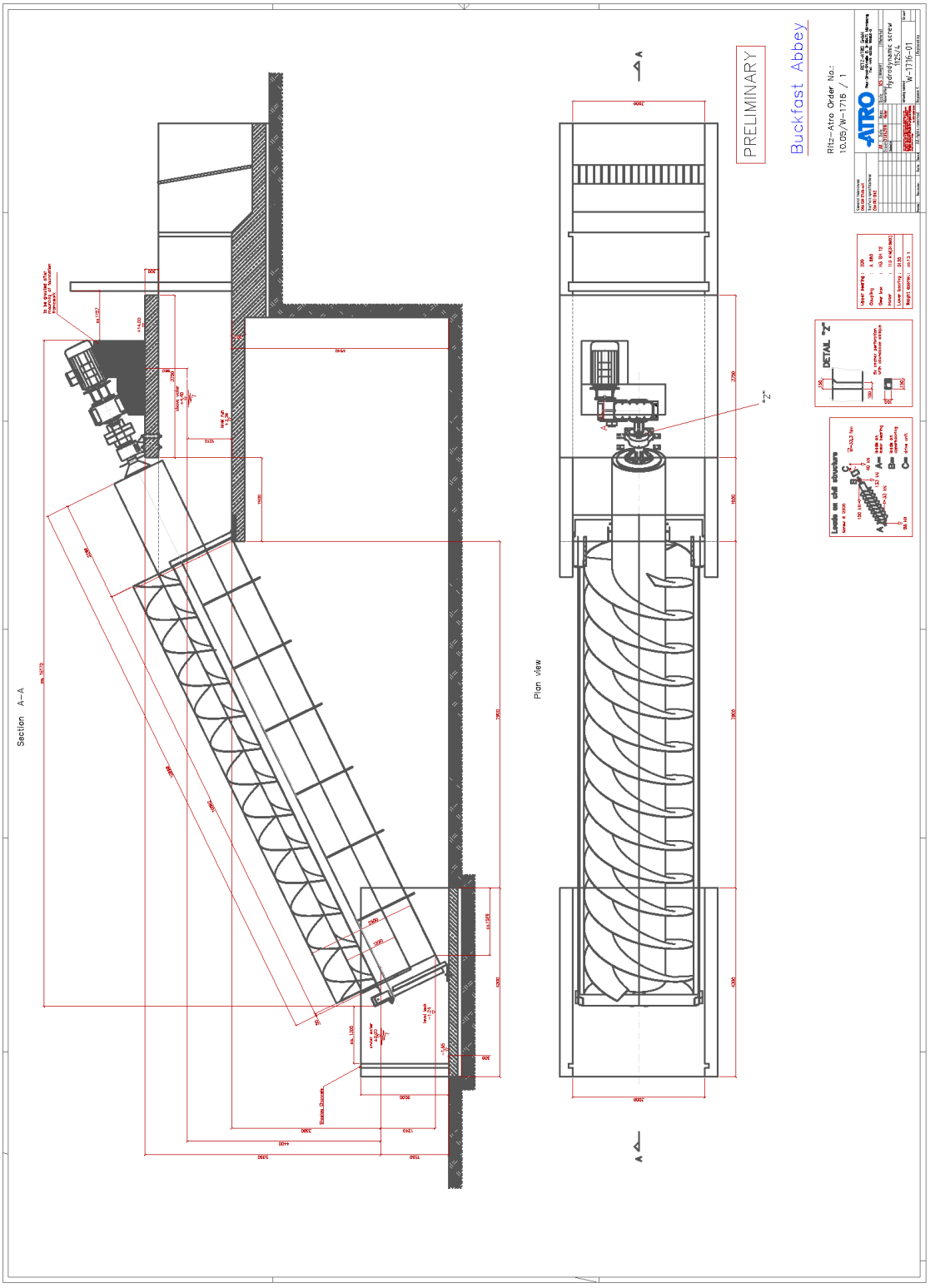

811
812 **Figure A 3: drawing of Buckfast Abbey installation.**

813

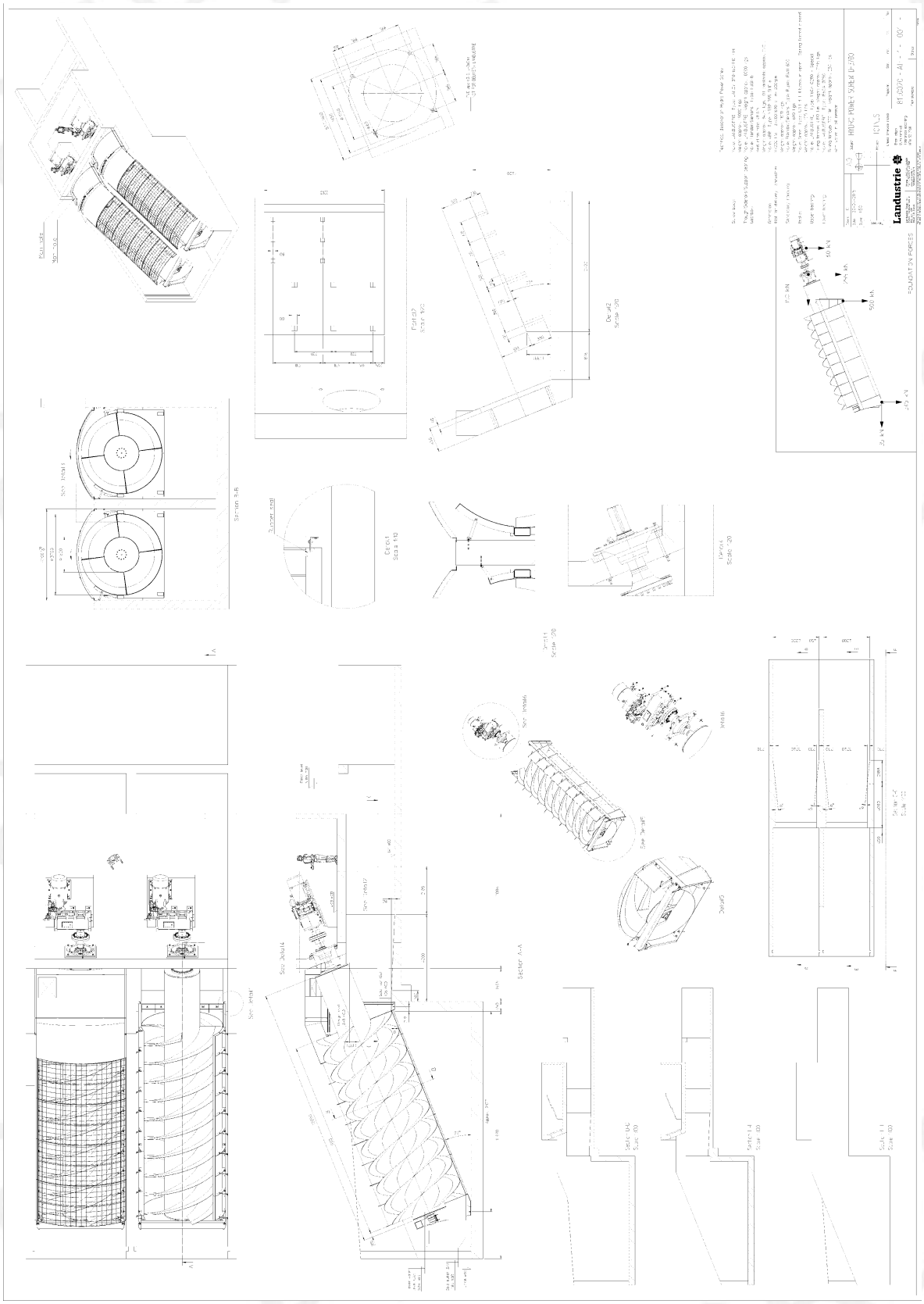

814

815 **Figure A 4: drawings of the Totnes installation.**